Inflammation, Vol. 45, No. 2, April 2022 (© 2022)
https://doi.org/10.1007/s10753-021-01574-0

ORIGINAL ARTICLE

Multiplex Immunofluorescence for Detection of Spatial Distributions of Infiltrating T Cells Within Different Regions of Hepatic Lobules During Liver Transplantation Rejection

Shi-peng Li[1,2,3], Guang-peng Zhou[1,2,3], Jie Sun[1,2,3], Bin Cui[1,2,3], Hai-ming Zhang[1,2,3], Lin Wei[1,2,3], Li-ying Sun[1,2,3,4] and Zhi-jun Zhu[1,2,3,4]

Received 10 May 2021; accepted 29 September 2021

Abstract—— It remains unclear as to whether there are differences that exist in the types and functional status of immune cells within different areas of the liver lobules after rejection of liver transplantation. The composition of infiltrating T cells in liver allografts during liver transplantation rejection is indistinct and difficult to visualize within the same biopsy slide. In an attempt to rectify this problem, we applied multiplex immunofluorescent assays to assess the spatial distribution of various types of infiltrating T cells in different areas of the liver lobules after liver transplantation. In identical areas of the hepatic lobules, the percentage of $CD4^+$ T, $CD8^+$ T, and regulatory T (Treg) cells in the rejection group was greater than that observed in the non-rejection and normal groups. Within all three groups, the percentage of $CD4^+$ T, $CD8^+$ T, and Treg cells from the periportal to perivenous zones initially increased and then decreased. In the rejection group, the percentage of $CD8^+$ T cells gradually increased from the periportal to perivenous zones, with maximal levels in the perivenous as compared with that in the transitional and periportal zones. In conclusion, levels of $CD8^+$ T cells within different regions of liver lobules are closely related to levels of rejection after liver transplantation. Liver transplantation rejection may be linked with increases in $CD8^+$ T cells within the perivenous zone. Although the regional percent of increase in $CD4^+$ T cells may not reflect level of the rejection, the overall numbers of both of $CD4^+$ and $CD8^+$ T cells within different regions were closely related to rejection levels.

KEY WORDS: spatial distribution; infiltrating T cells; hepatic lobule regions; liver transplantation rejection; multiplex immunofluorescence.

[1]Liver Transplantation Center, Clinical Research Center for Pediatric Liver Transplantation, National Clinical Research Center for Digestive Diseases, Beijing Friendship Hospital, Capital Medical University, Beijing 100050, China
[2]Clinical Research Center for Pediatric Liver, Transplantation of Capital Medical University, Beijing 100050, China
[3]National Clinical Research Center for Digestive Diseases, Beijing 100050, China
[4]To whom correspondence should be addressed at and Liver Transplantation Center, Clinical Research Center for Pediatric Liver Transplantation, National Clinical Research Center for Digestive Diseases, Beijing Friendship Hospital, Capital Medical University, Beijing, 100050, China. Email: sunliying@ccmu.edu.com; zhu-zhijun@outlook.com

INTRODUCTION

Rejection is a major obstacle to the long-term survival of liver grafts and prognosis of patients after liver transplantation [1, 2]. Rejection includes cell-mediated cell rejection and humoral antibody-mediated immune response [3]. Recent findings have indicated that changes in T cell subsets are associated within transplant rejection. Some examples of such T cell subsets include CD4$^+$ T cells, which can stimulate T cell clonal expansion and differentiation by recognizing allogeneic antigens and secrete interleukin (IL)-2. These cells can then induce acute rejection by activating CD8$^+$ cytotoxic T cells [4]. T helper (Th)17 cells, which are immune cells, mainly secrete IL-17A, IL-17F, and other cytokines to mediate the inflammatory responses [5]. T regulatory (Treg) cells represent another member of these T cell subsets. These cells play an important role in inhibiting transplantation immune rejection and induce immune tolerance [6]. Interestingly, the proportions of CD4$^+$ T, CD8$^+$ T and Th17 cells in the peripheral blood of patients with acute rejection is increased, while the proportion of Treg cells is increased in peripheral blood of patients without acute rejection [7]. Similar changes in CD4$^+$ T, CD8$^+$ T, Th17, and Tregs cells are observed in liver tissue.

To date, the exact phenotypes of these immune cells have not yet been specified. However, results from different phenotypic and molecular studies have suggested that the composition of the infiltrating lymphocytes may be an important factor as related to rejection. The liver consists of approximately 1 million hepatic lobules, and blood flows from the peripheral portal area to the central vein [8]. As there are gradient changes in nutrition, oxygen concentration, hormones, and other aspects in hepatocyte plates of the hepatic lobule, different metabolic functional areas are formed [9]. Hepatic lobules are divided into three regions according to their metabolic functions: perivenous, transitional, and periportal zones [8, 9]. Halpern et al. [10] divided the porto-central lobule axis into nine layers and developed a probabilistic inference algorithm to calculate the likelihood of each cell belonging to any of these layers based on the expression of our panel of landmark genes. The functional status of corresponding non-hepatic parenchymal cells (e.g., endothelial and immune cells) may be different due to the different partitions of the hepatic lobules.

It has been reported that Kupffer cells are enriched near periportal regions, with those closest to portal triads showing distinct phenotypic properties [11]. And there are quantitative data detailing this patterning, with MHCII^{hi} or MHCII^{int} Kupffer cells showing similar distances to the central vein [12]. These data reveal that the hepatic lobules contain a spatially polarized immune system, an "immune zonation." In contrast, the distribution of diverse resident immune cell types, the cellular and molecular mechanisms underlying the spatial organization of the liver immune system, and the functional consequences of asymmetric immune cell localization remain to be clarified. In specific, there are no reports regarding the spatial distribution of infiltrating T cells and changes in immune microenvironments within discrete areas of hepatic lobules during liver transplantation rejection. In part, this lack of information is due to the complexity of hepatic lobule structure, differences in gene expression patterns of the spatial axis from the central vein to the portal zone, and the gradual changes that occur in their function. This is especially problematic in the traditional hepatic lobule transitional zone, where many important genes are expressed. An intriguing related issue is whether differences exist in the types and functional status of immune cells within different regions of hepatic lobules. In response to this issue, we studied the infiltration and distribution of T cells in different regions of hepatic lobules under conditions of rejection versus non-rejection after liver transplantation.

While immunohistochemical or immunofluorescent techniques have been applied to detect changes in CD4 and CD8 cells as well as other indicators in grafts [13, 14], these techniques only reveal a certain type of T cell distribution as based on one or two indicators. Here, we employed a direct method that generated readouts consisting of a comprehensive panel of biomarkers from liver biopsies of liver transplantation patients. With multiplex immunofluorescent staining, it was possible to simultaneously label multi-cellular markers and, in this way, observe various cell types, their functional status, and interactions. Accordingly, critical details regarding the spatial localization of immune cells within different tissues are revealed to provide an enhanced comprehension of the immune microenvironment within organs and tissues [15]. Our findings indicate that infiltrated immune cells show spatial specificity which offers new insights into the changes which occur within discrete areas after liver transplantation. In specific, we found that the distribution of CD8$^+$ T cells within different regions of hepatic lobules was closely related to the rejection level, with rejection appearing to be associated with increases in the percentage of CD8$^+$ T cells in the perivenous zone.

Although the regional percent change in $CD4^+$ T cells does not appear to reflect the level of rejection, the overall numbers of both of $CD4^+$ T and $CD8^+$ T cells in different regions were closely related to the rejection level.

MATERIALS AND METHODS

Patients and Clinical Data Collection

Patients who underwent liver transplantation at the Liver Transplantation Center of the Beijing Friendship Hospital, Capital Medical University, over the period between January 2017 and July 2020 were included in this study. Demographic, medical, transplantation and follow-up data were obtained from all recipients (Table 1). Medical data included etiology of the liver disease and laboratory data. Data related to transplantation consisted of ABO blood group, donor sex and age, graft type, operation time, and warm ischemic time. Laboratory data included determinations of tacrolimus trough concentrations of tacrolimus and liver function tests such as albumin, aspartate aminotransferase (AST), alanine aminotransferase (ALT), and total bilirubin (TB). All liver grafts were voluntarily donated after cardiac death or by living donors, and all donations were approved by the Ethics Committee of the Beijing Friendship Hospital, Capital Medical University. Immunosuppressive regimens included intraoperative methylprednisolone and postoperative tacrolimus + mycophenolate mofetil + prednisone. Trough concentrations of tacrolimus were monitored after liver transplantation, and tacrolimus doses were adjusted according to post transplantation times and blood concentrations of tacrolimus.

Group Management of Liver Transplantation Patients

All liver transplantation patients were divided into either a rejection (R) or non-rejection (NR) group as based on the Banff schema for grading acute liver allograft rejections [16]. In addition, a normal group (N) was included. A total score of rejection activity index (RAI) was 9, and patients with scores < 3 were classified as non-rejection, while those with scores of 3–9 were considered rejection.

Liver Histology

Liver biopsies were performed using the Menghini method while patients were under deep propofol sedation [17]. Biopsies were performed by two experienced clinicians who used a 17-gauge needle to obtain a specimen of ≥ 2 cm in length. Normal liver tissues were obtained from living donors. The liver tissue samples were fixed in 4% mediosilicic isotonic formaldehyde for 24 h, dehydrated and embedded in paraffin. Sections (4-μm) were cut from each paraffin-embedded tissue and stained with hematoxylin and eosin (HE) to evaluate pathology of the liver.

Immunocytochemistry

Immunocytochemistry staining was used for determinations of protein expression and distribution after microwave treatment with a citrate antigen retrieval solution. Following incubation in 3% H_2O_2 for 10 min, antibodies against CD4 (Abcam, catalog number: ab133616, Cambridge, MA, USA), CD8 (Abcam, catalog number: ab237709, Cambridge, MA, USA), IL-17 (Abcam, catalog number: ab79056, Cambridge, MA, USA), and FOXP3 (Abcam, catalog number: ab22510, Cambridge, MA, USA) were added and incubated at 4 °C for 12 h. The specimens were incubated with secondary antibodies at 37 °C for 1 h, followed by diaminobenzidine staining. Negative controls (PBS instead of primary antibody) were run simultaneously with these samples.

Multiplex Immunofluorescent Assays [18]

Tissue multiplex immunofluorescent staining was performed using the Opal Polaris 5 color IHC staining kit (Akoya Biosciences). Briefly, formalin-fixed, paraffin-embedded (FFPE) tissue sections of (4 μm) were baked for 2 h at 60 °C before staining. Slides were rehydrated with a series of graded ethanol solutions in deionized water. Antigen retrieval was performed at pH 6 for 20 min at 95 °C. Slides were serially stained with the following antibodies: anti-CD4, -CD8, -IL-17, and -FOXP3. Anti-mouse/rabbit horseradish peroxidase (Cell Signaling Technology, Danvers, MA, USA) was used as the secondary antibody. TSA-conjugated fluorophores (PerkinElmer) were used to visualize each biomarker consisting of Opal 690 (IL-17), Opal 620 (FoxP3), Opal 570 (CD4), and Opal 520 (CD8) with incubation times for each primary antibody being 1 h. Subsequently, anti-rabbit/mouse Polymeric Horseradish Peroxidase (Opal IHC Detection Kit, Akoya Biosciences) was applied as a secondary label with an incubation time of 10 min.

Table 1 Baseline Characteristic of Liver Transplantation Recipients

Baseline characteristic	N1	N2	N3	R1	R2	R3	R4	NR1	NR2	NR3	NR4
Recipient											
Gender	Female	Male	Female	Female	Male	Female	Male	Female	Male	Female	Female
Age (yr)	27	25	24	0.58	0.58	60	14	0.67	45	23	45
ABO	O	O	B	A	B	O	O	B	O	A	O
AST (U/L)	12.3	11.4	23.6	141.7	86.1	267.4	27.7	26.7	28.9	14.7	29.5
ALT (U/L	7	11	13	118	50	181	20	17	23	5	18
Albumin (g/L)	45.3	42.4	45.8	34.7	40.1	27.9	43.3	44.5	41.8	40.3	41.4
Total bilirubin (μmol/L)	5.54	12.35	11.54	34.53	7.95	92.69	11.11	21.59	18.46	6.72	11.41
HBV-positive	NO	NO	NO	NO	NO	YES	NO	NO	YES	NO	YES
HCV-positive	NO	NO	NO	NO	NO	NO	NO	NO	NO	NO	NO
Etiology	-	-	-	Liver failure	Biliary atresia	Liver cirrhosis	Hepatoblastoma	Biliary atresia	hepatocellular carcinoma	Hyperoxaluria	Liver cirrhosis
Donor organ type	-	-	-	living donor	living donor	DCD	DCD	living donor	DCD	DCD	DCD
RAI	0	0	0	5	7	5	5	1	2	1	1
Donor											
Gender	-	-	-	Female	Female	Male	Male	Female	Male	Male	Male
Age (yr)	-	-	-	26	25	35	27	25	39	42	34
ABO	-	-	-	A	B	O	O	B	O	A	O
Cold ischemic time (h)	-	-	-	57 min	52 min	142 min	750 min	52 min	652 min	520 min	730 min
Warm ischemic time (min)	-	-	-	4 min	3 min	8 min	11 min	3 min	9 min	3 min	10 min

Antibody signals were visualized following a 10-min incubation period of the slides using the corresponding Opal Fluorophore (Akoya Biosciences). Slides were mounted with anti-fade mounting medium (P36965, Life Technologies) and stored at 4 °C before imaging. Image acquisitions (200 × magnification as multispectral images) were performed using the Vectra Polaris multispectral imaging platform (Akoya Biosciences), with the entire slide image being scanned and 3–5 representative regions of interest chosen by the pathologist. DAPI was used to count number of cells per slide. Again, negative controls (PBS instead of primary antibody) were run simultaneously with these samples.

Hepatic Lobule Zone

Hepatic lobules are divided into three regions: perivenous, transitional, and periportal zones, as previously described [8].

Statistical Analysis

The data were expressed as means ± standard deviation. Differences among the three groups were analyzed using a one-way analysis of variance and Newman-Keuls test for post hoc comparisons. SPSS version 22.0 was used for these analyses. A *P* value < 0.05 was required for results to be considered as statistically significant.

RESULTS

Pathological Changes in Liver

Histopathological features within the rejection group consisted of three major lesion components: inflammation of portal tracts, bile duct damage, and endotheliitis. A pleomorphic infiltration of lymphocytes, neutrophils, and plasma cells was observed within the portal tract. As compared with that of the normal group, considerable balloon-like degeneration, cholestasis, necrosis, phlebitis, and fibrosis were present in the rejection group. As compared with that of the non-rejection group, HE staining showed that the infiltrations of immune cells in portal areas and hepatic lobules were significantly increased in the rejection group. Moreover, bile duct and endothelial injury, along with hepatocyte edema and necrosis, were increased in this rejection versus non-rejection group (Fig. 1A).

Expressions and Distributions of CD4, CD8, IL-17, and FOXP3 in Liver Tissue

Different staining of CD4, CD8, IL-17 and FOXP3 in identical liver tissue section areas were determined with use of immunohistochemistry (Fig. 1B). CD4 was mainly expressed in the membrane and cytoplasm of sinusoidal endothelial cells, Kupffer cells, and lymphocytes. In the normal liver tissue of this report, CD4 was mainly expressed in liver sinusoidal endothelial cells, Kupffer cells, and T cells. Within the rejection group, infiltrating immune cells and $CD4^+$ T cells were significantly increased, while the number of $CD4^+$ liver sinusoidal endothelial cells and Kupffer cells were decreased. In the non-rejection group, infiltrating immune cells and $CD4^+$ T cells were significantly reduced, while the number of $CD4^+$ liver sinusoidal endothelial cells and Kupffer cells were increased. Overall, the expressions and distributions of $CD8^+$ T cells were similar to those of $CD4^+$ T cells. In normal liver tissue, there were few $CD8^+$ T cells, with the few present being mainly concentrated in the portal area, and very limited infiltration into hepatic lobules. In the rejection group, there was a significant increase in the number of $CD8^+$ T cells. In the non-rejection group, $CD8^+$ T cells were significantly decreased as compared with that of rejection group. IL-17 is mainly expressed in hepatocytes, endothelial cells, and immune cell cytoplasm. In the rejection group, there was an increased expression of IL-17 in lymphocytes as compared with that observed in the normal and non-rejection groups. Finally, FOXP3 is mainly expressed in nucleus and immune cells. $FOXP3^+$ T cells were almost not found in normal liver tissue. There were significantly more $FOXP3^+$ T cells than that in the non-rejection group.

Use of Multiplex Immunofluorescence to Measure Dynamic Changes in Infiltrating T Cells in Liver Rejection

Multiplexed immunofluorescent assays for CD4, CD8, IL-17, and FOXP3 were used as a means to visualize changes in the composition of immune infiltrates as associated with liver rejection (Fig. 2A). The proportion of various T cells types in each slice was calculated (N% = number of certain T cells/total number of cells in each slice × 100%), and differences in T cells among the three groups were compared. The results revealed that an increase in infiltrating $CD4^+$ T cells was observed in both the rejection and non-rejection groups as compared

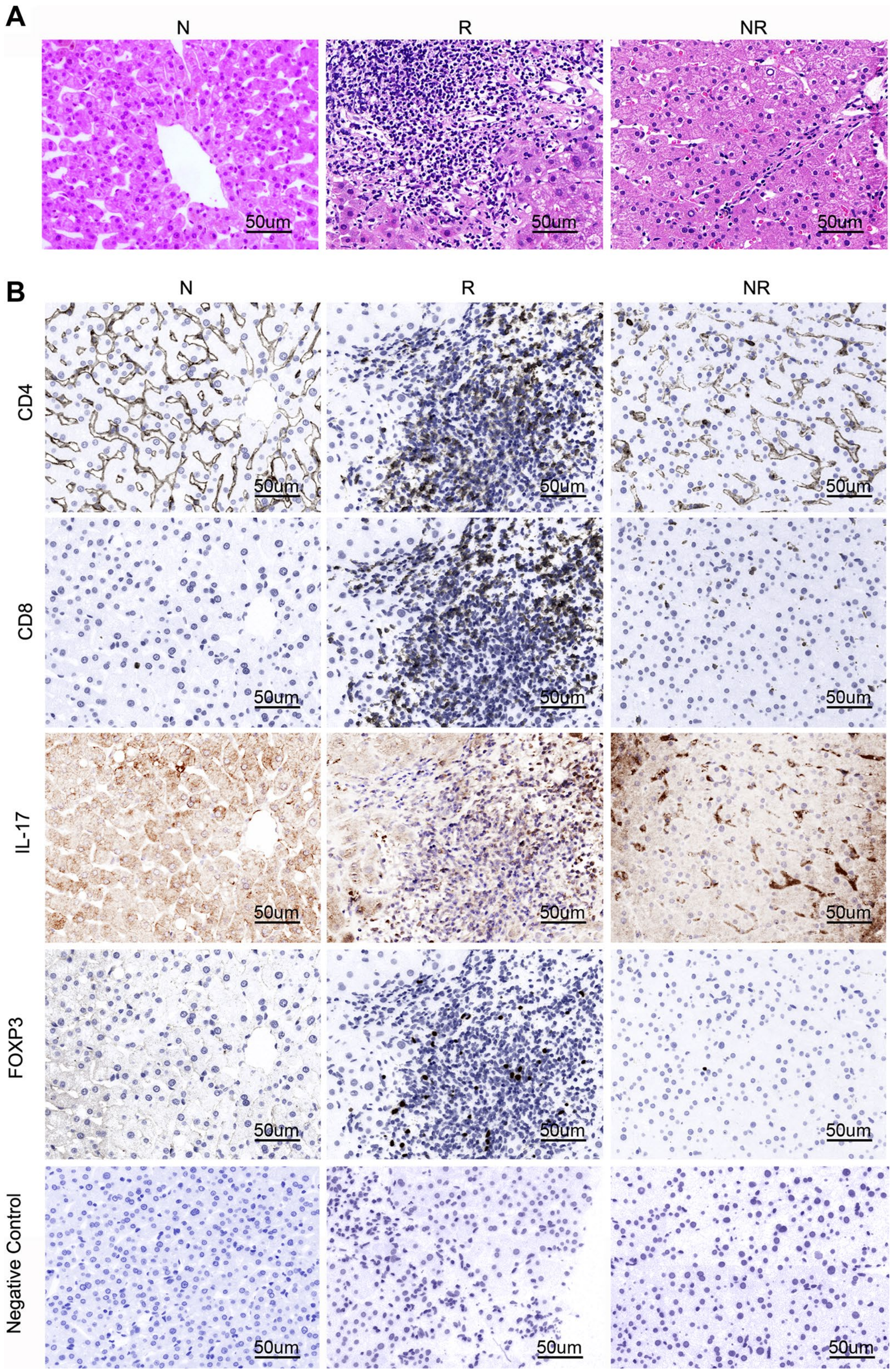
A
N
R
NR
50um
50um
50um
B
N
R
NR
CD4
CD8
IL-17
FOXP3
Negative Control
50um

◀**Fig. 1** Expressions of T cell related markers in liver tissue. **A** HE staining was used to observe pathological changes within liver tissue of each group (×200, scale bars = 50 μm). **B** Different staining of CD4, CD8, IL-17 and FOXP3 in identical liver tissue section areas in each group were detected with use of immunohistochemistry (×200, scale bars = 50 μm). Negative controls were simultaneously run with these samples.

with that of the normal group. Maximal and statistically significant levels of $CD4^+$ T cells were obtained in the rejection group (Fig. 2B, $P < 0.001$). The number of infiltrating $CD8^+$ T cells was highly variable among patients in there groups (Fig. 2C, $P < 0.001$). Infiltrating FOXP3 + regulatory T cells ($CD4^+FOXP3^+$ T and $CD8^+FOXP3^+$ T cells) were also observed in the liver. $CD4^+FOXP3^+$ T (Treg) and $CD8^+$FOXP3 + T cells were rarely observed in the livers of the normal and non-rejection groups, but statistically significant increases in the proportion of Treg and $CD8^+$ $FOXP3^+$ T cells were present in the rejection group (Fig. 2D and E, $P < 0.001$). We also found that the number of $CD4^+$IL-17^+ T (Th17) and $CD8^+$IL-17^+ T cells and the proportion of Th17 cells in the rejection group were significantly increased (Fig. 2F, $P < 0.001$). Although the overall number of $CD8^+$IL-17^+ T cells in liver tissue was low, the greatest proportion was present with in the rejection group (Fig. 2G, $P < 0.001$). Taken together, these results demonstrate that the proportions of $CD4^+$ T, $CD8^+$ T, Treg, and Th17 cells were all increased in rejection after liver transplantation, and suggest that these cells are involved in the formation of rejection or immune tolerance after liver transplantation. Under conditions of decreased levels or no rejection, these T cell types were either decreased or absent.

Distribution of Infiltrating T Cells in Hepatic Lobules and Portal Areas

Due to differences in the structure of hepatic lobules and portal areas (Fig. 3A and B), inflammatory cell infiltration distributions also differ. As achieved with the use of multiple staining techniques, we observed differences in T cell distribution in hepatic lobules and portal areas, and summarized the characteristics of T cell spatial distributions in the liver under different immune states of liver transplantation (Fig. 3C). In the normal group, few infiltrating T cells were present in the hepatic lobules, and only small number of $CD8^+$ T, $CD4^+$ T, $CD4^+$ $FOXP3^+$ T (Treg), and $CD4^+$ IL-17^+ T (Th17) cells were observed. In the rejection group, the number of infiltrating T cells including $CD8^+$ T cells was significantly increased. The number of infiltrating T lymphocytes in the non-rejection group was lower than that in the rejection group. While $CD8^+$ T and $CD4^+$ T cells were present in the non-rejection group, Treg and Th17 cells were rarely observed. In the normal group, infiltrating T cells were present in the portal area and mainly consisted of $CD8^+$ T and $CD4^+$ T cells, while a small number of Th17 but no Treg cells were observed. In the rejection group, infiltrating T cells were seen in the portal area, with large numbers of $CD8^+$ T and $CD4^+$ T cells, along with Treg and Th17 cells also being observed. The number of infiltrating T cells in non-rejection group was lower than that in the rejection group. While $CD8^+$ T and $CD4^+$ T cells were present in the non-rejection group, fewer Treg and Th17 cells were observed (Fig. 3C). These results show that the distribution of infiltrating T cells differs in terms of incidence as well as location of T cell types in the hepatic lobules and portal areas. In general, infiltrating T cells are mainly concentrated in the portal area, while relatively few infiltrate the hepatic lobules.

Distribution of T Cell Infiltration Within Different Areas of Hepatic Lobules

The hepatic lobule is divided into perivenous, transitional, and periportal zones (Fig. 4A and B). The percentage of $CD4^+$ T, $CD8^+$ T, and Treg cells in each region was statistically analyzed (n% = the number of T cells/total number of cells in the each zone × 100%), and differences in the percentage of these cells within each zone were compared among the three groups. Figure 4D contains a summary of the spatial distribution within the periportal zone of $CD4^+$ T, $CD8^+$ T, and Treg cells in the normal, rejection, and non-rejection groups. Results from multiplex immunofluorescent staining revealed that the percentage of Treg cells in the rejection group was significantly greater than that of the other two groups ($P < 0.001$). In addition, the percentage of $CD4^+$ T and $CD8^+$ T cells within both the rejection ($P < 0.01$) and non-rejection ($P < 0.05$) groups were greater than that in the normal group. While the percentage of $CD4^+$ T cells in the non-rejection group was significantly decreased versus that in the rejection group, these levels were significantly increased over that in the normal group ($P < 0.05$). In the transitional zone, the percentage of $CD4^+$ T and Treg cells in the rejection group was significantly increased over that of the other two groups

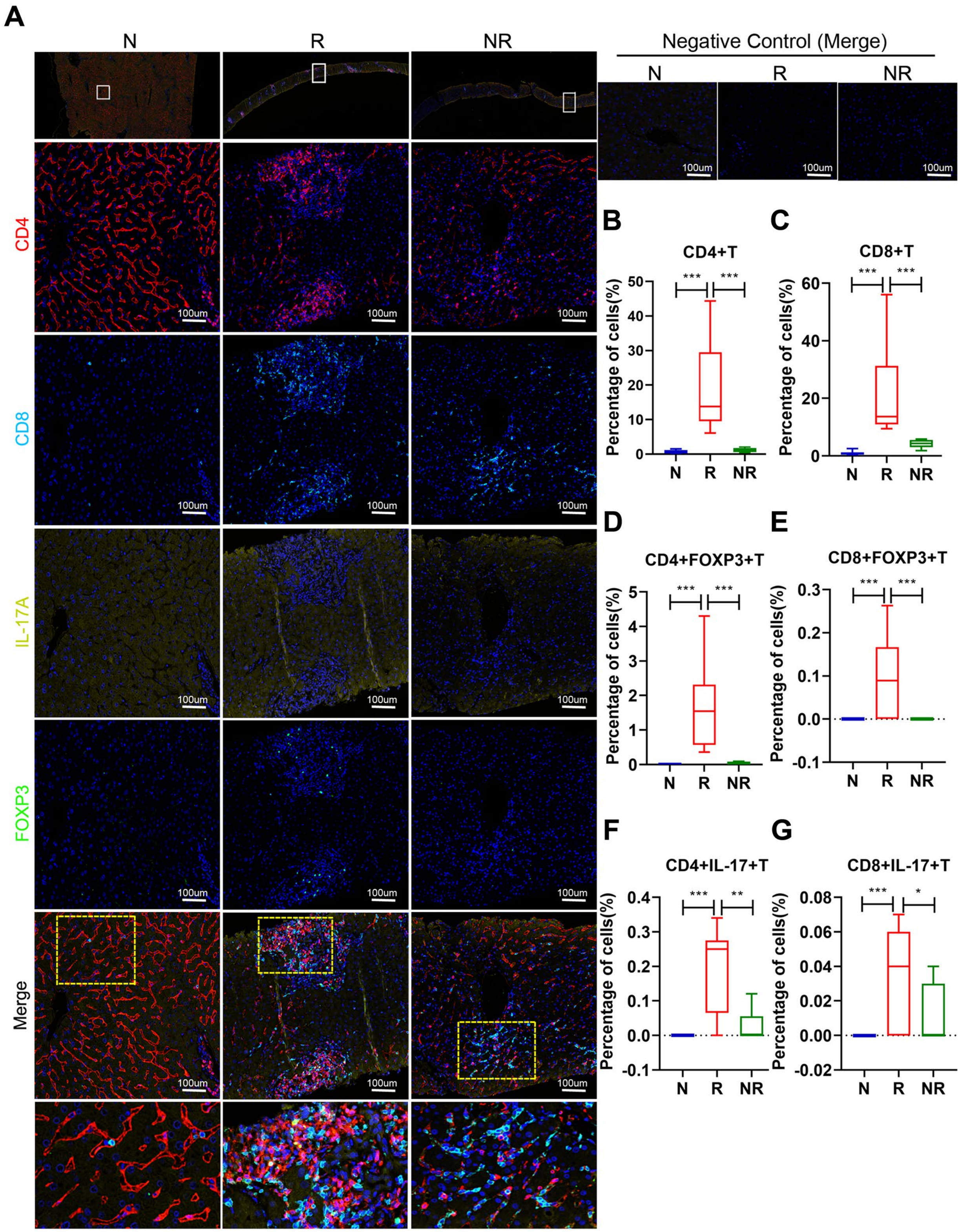
A
N
R
NR
Negative Control (Merge)
CD4
CD8
IL-17A
FOXP3
Merge
100um
B
CD4+T
C
CD8+T
D
CD4+FOXP3+T
E
CD8+FOXP3+T
F
CD4+IL-17+T
G
CD8+IL-17+T
Percentage of cells(%)

◂**Fig. 2** Increased T-cell infiltration was related to rejection after liver transplantation. **A** Multiplexed immunofluorescent staining of immune cell marker panels (CD4-red, CD8-light blue, IL-17-yellow, FOXP3-green) and DAPI (blue) of liver tissue in each group (×200, scale bars = 100 μm). **B** The percentage of $CD4^+T$, $CD8^+T$, $CD4+FOXP3^+T$, $CD8^+FOXP3^+T$, $CD4^+IL\text{-}17^+T$, and $CD8^+$ IL-17 + T cells within liver tissue of each group. Negative controls were simultaneously run with these samples. $^*P<0.05$, $^{**}P<0.01$, $^{***}P<0.001$ compared with R group.

($P<0.01$) and the percentage of $CD8^+$ T cells was greater than that of the normal group ($P<0.05$). Within this zone, a significantly greater percentage of $CD4^+$ T cells obtained in the rejection group was significantly higher than in the non-rejection group ($P<0.05$). Overall, the percentage of $CD4^+$ T, $CD8^+$ T, and Treg cells was significantly lower in the rejection group as compared with the normal group ($P<0.05$). In the perivenous zone, the proportion of $CD4^+$ T, $CD8^+$ T, and Treg cells in the rejection group was found to be significantly increased as compared with the other two groups ($P<0.05$). The percentage of $CD4^+$ T and $CD8^+$ T cells in the non-rejection group was significantly lower than that in the rejection group, but significantly higher as compared with that in the normal group ($P<0.05$).

We also observed differences in T cell spatial distributions within different regions of liver tissue in the same group (Fig. 4E). While varying percentage of $CD4^+$ T cells and Treg cells were observed within different regions in the normal group, these differences failed to achieve statistical significance ($P>0.05$). In the transitional zone of the normal group, the percentage of $CD4^+$ T cells was significantly higher than that of the other two regions ($P<0.05$). In the rejection group, the percentage of $CD4^+$ T cells from the periportal to perivenous zones was not statistically different ($P>0.05$), while the percentage of $CD8^+$ T cells showed a gradual increase from the periportal to perivenous zones, with a statistically significant increased being obtained in this perivenous versus the other two zones ($P<0.05$). In this rejection group, the percentage of Treg cells in the transitional zone was significantly greater than that observed in the perivenous zone ($P<0.05$). For the non-rejection group, the percentage of $CD4^+$ T and $CD8^+$ T cells from the periportal to perivenous zones failed to achieve a statistically significant difference ($P>0.05$), while the percentage of Treg cells in the transitional zone was found to be significantly greater than that obtained in the other two regions ($P<0.05$).

DISCUSSION

T cells play an important role in the rejection of allogeneic liver transplantation [19], through their capacity to participate in the recognition of transplantation antigens, immune regulation, cell dissolving effects, and other immune responses [20, 21]. In order to assess the phenotype and quantity of T cells as associated with different levels of liver rejection, changes in $CD4^+$ T, $CD8^+$ T, Treg, and Th17 cells in peripheral blood were determined using flow cytometry or immunohistochemistry. Following liver transplantation, the blood levels of $CD4^+$ T cells were maximal in the rejection group and significantly higher than that observed in the non-rejection group [22]. Treg and Th17 cells are known to be involved in alloreactive responses of organ transplantation. Wang et al. [23] investigated whether the circulating Treg/Th17 ratios were associated with acute allograft rejection in liver transplantation. Under conditions of rejection, the frequency of circulating Treg cells was significantly decreased, whereas the frequency of circulating Th17 cells was significantly increased. The Treg/Th17 ratio shows a negative correlation with liver damage indices and scores of rejection activity index after liver transplantation.

With immune rejection, large numbers of T cells, such as CD4 and CD8 subsets, infiltrate the graft, which enhances the aggravation of rejection [24]. The most notable histological changes associated with rejection involve mixed inflammatory cell infiltration of the confluence area [25]. Krukemeyer et al. [26] reported that greater numbers of B lymphocytes and plasma cells migrated to the liver in patients experiencing rejection as compared with that in non-rejection patients. However, the experimental techniques used in that study have some limitations, as the exact composition of leukocyte infiltration during allograft liver rejection was difficult to comprehend and visualize in the same biopsy slide. Some of these limitations have been resolved with the developments in science and technology, in particular, multiplex immunofluorescent assays.

Recent advances in multiplexed imaging platforms have enabled the simultaneous detection of multiple epitopes in the same tissue, which has thus emerged as a powerful tool for the study of the immune context of organs and tissues [27]. In specific, multiplex immunofluorescent assays can serve as a means to significantly improve the understanding of tissue microenvironments, which can then aid in the identification of new therapeutic targets and prognostic and predictive biomarkers, as well

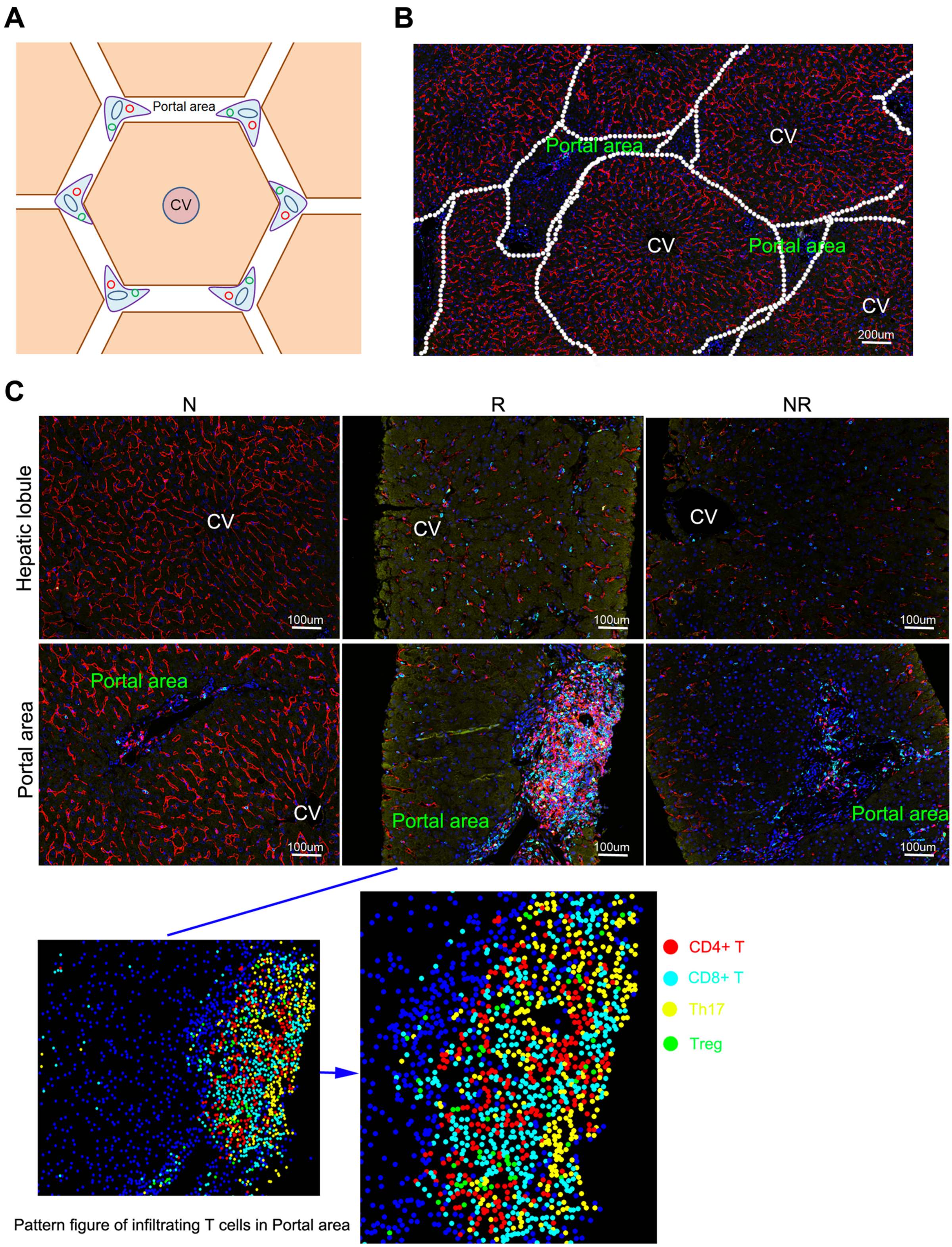
A
Portal area
CV
B
Portal area
CV
CV
Portal area
CV
200um
C
N
R
NR
Hepatic lobule
CV
100um
CV
100um
CV
100um
Portal area
Portal area
CV
100um
Portal area
100um
Portal area
100um
CD4+ T
CD8+ T
Th17
Treg
Pattern figure of infiltrating T cells in Portal area

◀**Fig. 3** Distribution of infiltrating T cells in hepatic lobules and portal areas. **A** Pattern of hepatic lobules and portal areas. **B** Schematic diagram of boundary between hepatic lobules and portal area (×200, scale bars = 100 μm). **C** Multiplexed immunofluorescent staining of immune cell marker panel (CD4-red, CD8-light blue, IL-17-yellow, FOXP3-green) and DAPI (blue) in hepatic lobules and portal areas in each group (×200, scale bars = 100 μm).

as in the development of translational studies [28]. Prior to this current report, this new technology was mainly used in oncology studies to better characterize in situ immune cell infiltration in tumors [29–31]. When immunohistochemical or immunofluorescent techniques have been applied to detect changes in $CD4^+$ T, $CD8^+$ T, Th17, and Treg cells as well as other indicators in grafts, these serial tissue sections make it difficult to analyze the cellular interplay and precise location of these cells. In contrast, with present multiplex immunofluorescent assays, it is possible to generate readouts for a comprehensive panel of biomarkers from liver biopsies of liver transplantation patients. Our findings reveal that increased infiltrations of $CD4^+$ T and $CD8^+$ T cells were present in both the rejection and non-rejection groups as compared with that in the normal group, with the rejection group showing the highest proportions of these cells. In addition, although it was difficult to observe Treg cells in the normal and non-rejection groups, the proportion of Treg and Th17 cells were maximal in the rejection group. These results, demonstrating that the proportions of $CD4^+$ T, $CD8^+$ T, Treg, and Th17 cells were all increased with rejection after liver transplantation, suggest that these cells were involved in the development of rejection or immune tolerance after liver transplantation. With the use of multiplex immunofluorescent assays, Calvani et al. [32] were able to simultaneously detect NK cells, macrophages, and T cells to determine their intra- or extra-vascular localization in kidney allograft rejections. Accordingly, that study demonstrated the feasibility and utility of applying multiplex immunofluorescent imaging to study and better understand these cells along with their discrete localizations as associated with the rejection process. The results of this study show that different types of lymphocytes are associated with differential immune state infiltrations after organ transplantation and thus reveal that the mechanisms through which different immune cells participate in rejection or immune tolerance can be quite diverse.

With acute rejection, interlobular bile ducts and vascular endothelial cells represent the primary targets of immune assault [33]. Many immune cells infiltrate the mixed portal area and hepatic lobules, which results in venous endothelial and bile duct inflammations [34]. Similarly, our immunofluorescent staining results showed that infiltrating T cells were observed in the portal area in the rejection group and included large numbers of $CD8^+$ T, $CD4^+$ T, Treg, and Th17 cells. In contrast, the number of infiltrating T lymphocytes in the non-rejection group was significantly less than that in the rejection group. We also observed the novel phenomenon that the amount of lymphocyte infiltration within hepatic lobules was related to the level of rejection, while the number of CD4 + sinusoidal endothelial and Kupffer cells decreased significantly. The exact function and role of these $CD4^+$ sinusoidal endothelial and Kupffer cells is indefinite due to the lack of relevant research on this topic. In particular, the role of $CD4^+$ sinusoidal endothelial cells and Kupffer cells in the process of liver transplant rejection or immune tolerance is unknown. Results from previous studies have demonstrated that tissue-resident immune cells are important for organ homeostasis and defense and their epithelia may contribute to these functions either directly or via cross-talk with immune cells [35]. The mechanisms of interaction between T cells and sinusoidal endothelial cells in rejection of liver transplantation require further study.

Our results reveal the differential distribution of infiltrating T cells that occurs within hepatic lobules and portal areas. Due to the complexity of the hepatic lobule, this structure can be divided into three regions according to the different metabolic functions found in these regions. Interestingly, the variations in gene expression patterns of the spatial axis from the central vein to portal area are accompanied with ongoing variations in function [10]. As liver lobules contain a spatially polarized immune system, an "immune zonation," the types and numbers of immune cells infiltrating hepatic lobules differ as a function of the specific disease state [12]. For example, Kupffer cells can localize infiltrating neutrophils to the periportal regions of the lobule, thereby limiting damage to cells that reside around the central vein [36]. Whether differences are present in the types and functional status of immune cells within different regions of hepatic lobules under varying conditions of rejection remains unclear. In an attempt to assess this possibility, we used multiple immunofluorescent staining to examine the infiltration and spatial distribution of various types of T cells within different areas of hepatic lobules under conditions of rejection versus non-rejection after liver transplantation. Our results revealed that infiltrated immune cells do, in fact, demonstrate varying degrees of spatial specificity after liver transplantation.

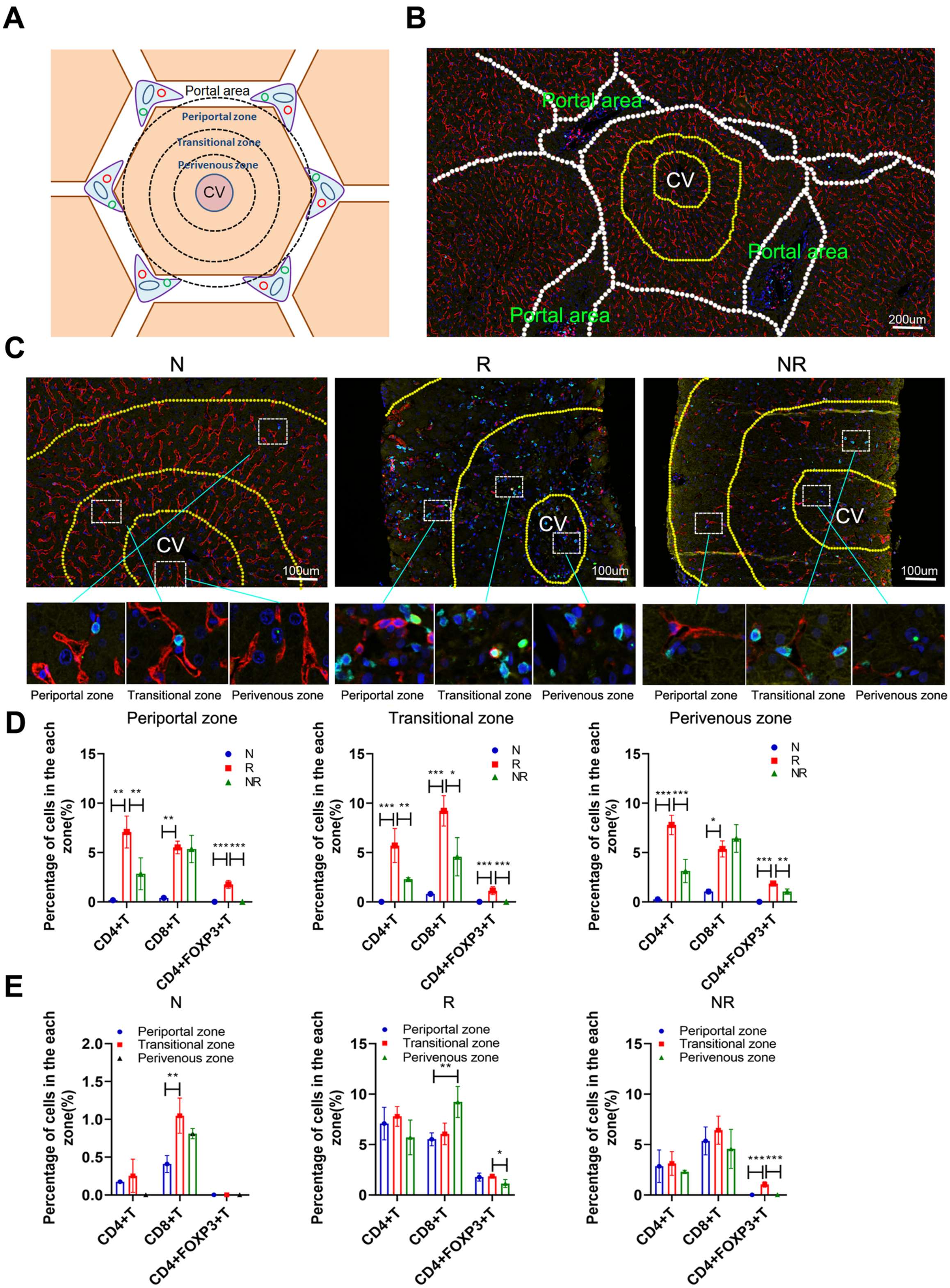
A
B
C
D
E
Portal area
Periportal zone
Transitional zone
Perivenous zone
CV
200um
100um
N
R
NR
Periportal zone
Transitional zone
Perivenous zone
Percentage of cells in the each zone(%)
CD4+T
CD8+T
CD4+FOXP3+T

◂**Fig. 4** Distribution of infiltrating T cells in different regions of hepatic lobules. **A** Pattern of hepatic lobular divisions. **B** Schematic diagram of boundary among divisions of hepatic lobules. **C** Multiplexed immunofluorescent staining of immune cell marker panels (CD4-red, CD8-light blue, IL-17-yellow, FOXP3-green) and DAPI (blue) in perivenous, transitional, and periportal zones (×200, scale bars = 100 μm). **D** Percent of $CD4^+$T, $CD8^+$T, and $CD4^+FOXP3^+$ T cells within each area (periportal, transitional or perivenous zone) in N, R and NR groups (×200, scale bars = 100 μm). *$P < 0.05$, **$P < 0.01$, ***$P < 0.001$ compared with R group. **E** Within the same group (N, R or NR group), the percentage of $CD4^+$T, $CD8^+$T, and $CD4^+FOXP3^+$ T cells in periportal, transitional, or perivenous zone (×200, scale bars = 100 μm). *$P < 0.05$, ***$P < 0.001$ compared with transitional zone.

In specific, within identical areas of the hepatic lobule, the percentage of $CD4^+$ T, $CD8^+$ T, and Treg cells in the rejection group was greater than that observed in the normal and non-rejection groups. These findings demonstrate the discriminatory increases in these T cells within the hepatic lobule that result in response to rejection. Within all three groups, the percentage of $CD4^+$ T, $CD8^+$ T, and Treg cells from the periportal zone to perivenous zone initially increased and then decreased. Interestingly, the percentage of $CD8^+$ T cells from the periportal to perivenous zones increased gradually, with maximal levels of these cells being observed in the perivenous zone of the rejection group. It has been reported that in kidneys, renal allograft biopsies with c-aABMR show a predominance of infiltrating $CD8^+$ T cells, and increased numbers of interstitial $FOXP3^+$ T cells are associated with inferior allograft survival [37]. Similarly, the distribution of $CD8^+$ T cells in different regions of hepatic lobules, as observed in this current investigation, may be closely related to the level rejection after liver transplantation.

There are some limitations in our study. The limited number of clinical samples, difficulty in obtaining liver biopsy specimens, and the incomplete structure of hepatic lobules from liver biopsy tissue represent some of the more salient limitations. Therefore, future work in this area will require procedures directed at resolving these issues. In conclusion, our results suggest that the percentage of $CD8^+$ T cells within different regions of hepatic lobules is closely related to the level of rejection that can occur after liver transplantation. We observed a significant degree of heterogeneity in the global composition of inflammatory burdens during liver allograft rejection. In specific, we found that rejection of liver transplantation was associated with increases in the percentage of $CD8^+$ T and Treg cells in the perivenous region. Moreover, the number and proportion of $CD8^+$ T cells gradually increased from the periportal to perivenous zones as a function of the degree of rejection. Although regional changes in the percentage of $CD4^+$ T cells did not appear to reflect the level of rejection, the overall numbers of $CD4^+$ and $CD8^+$ T cells within different regions were closely related to the level of rejection.

ACKNOWLEDGEMENTS

The authors would like to thank the Key Laboratory of Transplantation immunity of Beijing for their technical support.

AUTHOR CONTRIBUTION

Shi-peng Li and Zhi-jun Zhu contributed to the research design. Guang-peng Zhou, Jie Sun, and Bin Cui collected the clinical data; Shi-peng Li and Jie Sun performed multiplex immunofluorescent assays and immunocytochemistry. Hai-ming Zhang, Lin Wei, and Li-ying Sun contributed to the data management and statistical analyses. Shi-peng Li and Zhi-jun Zhu wrote the manuscript. Shi-peng Li and Guang-peng Zhou contributed equally to this work.

FUNDING

This work was supported by the National Natural Science Foundation of China (No. 81970562).

DECLARATIONS

Ethics Approval and Consent to Participate The study protocol was approved by the ethics committee of Beijing Friendship Hospital, Capital Medical University, Beijing, China.

Consent for Publication All authors have reviewed the manuscript and have given consent for publication.

Availability of Data and Materials All data generated or analyzed during this study are available in this article.

Competing Interests The authors declare no conflicts of interest in this work.

REFERENCES

1. Taner, T. 2017. Liver transplantation: Rejection and tolerance. *Liver Transplantation* 23 (S1): S85–S88.
2. Wei, Q., K. Wang, Z. He, et al. 2018. Acute liver allograft rejection after living donor liver transplantation: Risk factors and patient survival. *American Journal of the Medical Sciences* 356 (1): 23–29.

3. Duizendstra, A.A., M. Doukas, M. Betjes, et al. 2021. HLA matching and rabbit antithymocyte globulin as induction therapy to avoid multiple forms of rejection after a third liver transplantation. *Clinics and Research in Hepatology and Gastroenterology* 45 (3): 101539.
4. Chen, X., J. Zheng, J. Cai, et al. 2017. The cytoskeleton protein beta-actin may mediate T cell apoptosis during acute rejection reaction after liver transplantation in a rat model. *American Journal of Translational Research* 9 (11): 4888–4901.
5. Xie, X.J., Y.F. Ye, L. Zhou, et al. 2010. Th17 promotes acute rejection following liver transplantation in rats. *Journal of Zhejiang University. Science. B* 11 (11): 819–827.
6. Le Moine, A. 2021. What are the effects of everolimus and basiliximab on Tregs regulation and tolerance after liver transplantation? *Clinics and Research in Hepatology and Gastroenterology* 45 (5): 101591.
7. Haarer, J., P. Riquelme, P. Hoffmann, et al. 2016. Early enrichment and restitution of the peripheral blood tregs pool is associated with rejection-free stable immunosuppression after liver transplantation. *Transplantation* 100 (7): e39-40.
8. Steiner, P.E., and H.L. Ratcliffe. 1968. The hepatic lobules of suidae, tayassuidae, and hippopotamidae. *Anatomical Record* 160 (3): 531–538.
9. Chikamori, K., T. Araki, and M. Yamada. 1985. Pattern analysis of the heterogeneous distribution of succinate dehydrogenase in single rat hepatic lobules. *Cellular and Molecular Biology* 31 (3): 217–222.
10. Halpern, K.B., R. Shenhav, O. Matcovitch-Natan, et al. 2017. Single-cell spatial reconstruction reveals global division of labour in the mammalian liver. *Nature* 542 (7641): 352–356.
11. Sleyster, E.C., and D.L. Knook. 1982. Relation between localization and function of rat liver Kupffer cells. *Laboratory Investigation* 47 (5): 484–490.
12. Gola, A., M.G. Dorrington, E. Speranza, et al. 2021. Commensal-driven immune zonation of the liver promotes host defence. *Nature* 589 (7840): 131–136.
13. Okamura, A., T. Matsushita, A. Komuro, et al. 2020. Adipose-derived stromal/stem cells successfully attenuate the fibrosis of scleroderma mouse models. *International Journal of Rheumatic Diseases* 23 (2): 216–225.
14. Chen, Z., J. Liu, and D. Xu. 2021. Oncolytic adenovirus expressing CCL19 enhances immunity against gastric cancer in mice. *Xi Bao Yu Fen Zi Mian Yi Xue Za Zhi* 37 (2): 119–124.
15. Mauldin, I.S., A. Mahmutovic, S.J. Young, and C.J. Slingluff. 2021. Multiplex immunofluorescence histology for immune cell infiltrates in melanoma-associated tertiary lymphoid structures. *Methods in Molecular Biology* 2265: 573–587.
16. Demetris, A.J., C. Bellamy, S.G. Hubscher, et al. 2016. 2016 Comprehensive update of the banff working group on liver allograft pathology: Introduction of antibody-mediated rejection. *American Journal of Transplantation* 16 (10): 2816–2835.
17. Rasmussen, S.N., H.H. Holm, J.K. Kristensen, and H. Barlebo. 1972. Ultrasonically-guided liver biopsy. *British Medical Journal* 2 (5812): 500–502.
18. Canadas, I., R. Thummalapalli, J.W. Kim, et al. 2018. Tumor innate immunity primed by specific interferon-stimulated endogenous retroviruses. *Nature Medicine* 24 (8): 1143–1150.
19. Crosbie, O.M., S. Norris, J.E. Hegarty, and C. O'Farrelly. 1998. T lymphocyte subsets and activation status in patients following liver transplantation. *Immunological Investigations* 27 (4–5): 237–241.
20. Natsuda, K., S. Eguchi, M. Takatsuki, et al. 2016. CD4 T lymphocyte counts in patients undergoing splenectomy during living donor liver transplantation. *Transplant Immunology* 34: 50–53.
21. Jiang, Z., Y. Chen, X. Feng, et al. 2013. Recipient cytotoxic T lymphocyte antigen 4 +49 single-nucleotide polymorphism is not associated with acute rejection after liver transplantation in Chinese population. *International Journal of Medical Sciences* 10 (3): 250–254.
22. Dong, J.Y., H. Yin, R.D. Li, et al. 2011. The relationship between adenosine triphosphate within CD4(+) T cells and acute rejection after liver transplantation. *Clinical Transplantation* 25 (3): E292–E296.
23. Wang, Y., M. Zhang, Z.W. Liu, et al. 2014. The ratio of circulating regulatory T cells (Tregss)/Th17 cells is associated with acute allograft rejection in liver transplantation. *Plos One* 9 (11): e112135.
24. Kamada, N., H.S. Davies, D. Wight, L. Culank, and B. Roser. 1983. Liver transplantation in the rat. Biochemical and histological evidence of complete tolerance induction in non-rejector strains. *Transplantation* 35 (4): 304–311.
25. Qian, S., L. Lu, Y. Li, et al. 1997. Apoptosis of graft-infiltrating cytotoxic T cells: A mechanism underlying "split tolerance" in mouse liver transplantation. *Transplantation Proceedings* 29 (1–2): 1168–1169.
26. Krukemeyer, M.G., J. Moeller, L. Morawietz, et al. 2004. Description of B lymphocytes and plasma cells, complement, and chemokines/receptors in acute liver allograft rejection. *Transplantation* 78 (1): 65–70.
27. Lee, C.W., Y.J. Ren, M. Marella, et al. 2020. Multiplex immunofluorescence staining and image analysis assay for diffuse large B cell lymphoma. *Journal of immunological methods* 478: 112714.
28. Francisco-Cruz, A., E.R. Parra, M.T. Tetzlaff, and I.I. Wistuba. 2020. Multiplex immunofluorescence assays. *Methods in Molecular Biology* 2055: 467–495.
29. Viratham, P.A., S.G. Craig, V. Bingham, et al. 2020. A robust multiplex immunofluorescence and digital pathology workflow for the characterisation of the tumour immune microenvironment. *Molecular Oncology* 14 (10): 2384–2402.
30. Parra, E.R., N. Uraoka, M. Jiang, et al. 2017. Validation of multiplex immunofluorescence panels using multispectral microscopy for immune-profiling of formalin-fixed and paraffin-embedded human tumor tissues. *Science and Reports* 7 (1): 13380.
31. Parra, E.R., J. Zhai, A. Tamegnon, et al. 2021. Identification of distinct immune landscapes using an automated nine-color multiplex immunofluorescence staining panel and image analysis in paraffin tumor tissues. *Science and Reports* 11 (1): 4530.
32. Calvani, J., M. Terada, C. Lesaffre, et al. 2020. In situ multiplex immunofluorescence analysis of the inflammatory burden in kidney allograft rejection: A new tool to characterize the alloimmune response. *American Journal of Transplantation* 20 (4): 942–953.
33. Porter, K.A. 1969. Pathology of liver transplantation. *Transplantation Reviews* 2: 129–170.
34. Lefkowitch, J.H. 2002. Diagnostic issues in liver transplantation pathology. *Clinics in liver disease* 6 (2): 555–570.
35. Stewart, B.J., J.R. Ferdinand, M.D. Young, et al. 2019. Spatiotemporal immune zonation of the human kidney. *Science* 365 (6460): 1461–1466.
36. Halpern, K.B., R. Shenhav, H. Massalha, et al. 2018. Paired-cell sequencing enables spatial gene expression mapping of liver endothelial cells. *Nature Biotechnology* 36 (10): 962–970.
37. Sablik, K.A., E.S. Jordanova, N. Pocorni, G.M. Clahsen-van, and M. Betjes. 2019. Immune cell infiltrate in chronic-active antibody-mediated rejection. *Frontiers in Immunology* 10: 3106.